Mountain Basin Hydrologic Study

Douglas D. Woolridge
Jeffrey D. Niemann

Department of Civil and Environmental Engineering
Colorado State University

December 2018

Colorado Water Institute

Colorado State University

Abstract:
A long-standing problem for the Rocky Mountain region is that traditional meteorology and flood hydrology methods appear to significantly overestimate floods based on comparisons to paleoflood evidence and regional peak streamflow statistics. The Colorado Water Conservation Board (CWCB), Colorado Division of Water Resources (DWR), and state of New Mexico are conducting a $1.5 million study to develop improved estimates of extreme precipitation for the two-state region. Concurrently, DWR has been working to improve flood hydrology methods for the mountain region. Traditional flood hydrology methods utilize low infiltration rates to model flood runoff solely by an infiltration-excess mechanism. However, a recent but preliminary examination of the Gross Reservoir Basin suggests that saturation-excess runoff might be important for extreme precipitation events. The objectives of this research project are: (1) to determine the importance of saturation-excess runoff production for large storms that affect the design and performance of dams and transportation infrastructure and (2) to develop a generalized model for runoff production in mountainous basins that can be used by consultants to perform hydrologic analysis of dams and transportation infrastructure. In-situ soil moisture observations indicate that south-facing slopes often reached saturation during the September 2013 flood while north-facing slopes usually did not. They further suggest that saturation occurred first at the bottom of the soil layer and proceeded upward. These observations are consistent with saturation-excess runoff production. The preliminary model results also indicate that saturation-excess runoff production was the primary runoff production mechanism in South Boulder Creek during the September 2013 flood. Additionally, the model results show that south-facing slopes approached saturation while the north-facing slopes did not.

Keywords:
September 2013, floods, extreme events, runoff production, infiltration-excess, saturation-excess, hydrologic response, South Boulder Creek, Gross Reservoir

Table of Contents:

List of Figures:

List of Tables:

1. JUSTIFICATION OF WORK PERFORMED

The safety of Colorado's dams is critical for the protection of human life and prevention of economic and environmental losses. Spillway regulations are based on extreme flows that a given dam might encounter, and such flows are produced by the combination of extreme precipitation and the conversion of precipitation into runoff and streamflow. An important and long-standing problem for the Rocky Mountain region is that traditional rainfall-runoff modeling methods appear to significantly overestimate major floods based on comparisons to paleoflood evidence and regional peak streamflow statistics (Jarrett and Costa, 1988). The Colorado Water Conservation Board (CWCB), Colorado Division of Water Resources (DWR), and state of New Mexico are currently conducting a $1.5 million study to develop improved estimates of extreme rainfall for the two state region. DWR has also been working to improve flood hydrology methods for the Rocky Mountain region. Solving this problem would allow higher confidence in dam design, more efficient allocation of repair and replacement funds, and streamlined design guidelines.

Traditional flood hydrology methods utilize low infiltration rates to model flood runoff solely by an infiltration-excess mechanism. By this mechanism, runoff occurs when the rainfall intensity exceeds the infiltration capacity of the soil. However, forested basins typically have soils with high infiltration capacities that produce little infiltration-excess runoff (Dunne and Leopold, 1978; Dunne, 1978; MacDonald and Stednick, 2003; Whipkey, 1965). Furthermore, the bedrock geology and weathering processes of many mountain basins leads to coarse soils with high infiltration rates.

Recent advances by DWR indicate that flood runoff in mountain basins might be controlled by a saturation-excess mechanism (DWR, 2014 and 2015). Saturation-excess runoff can occur when a relatively shallow soil is underlain by a layer with much lower permeability (usually bedrock), which is a relatively common situation in Rocky Mountain basins (Dunne, 1978). Rainfall rates that are less than the infiltration capacity can still produce runoff if the storm continues long enough to saturate the thin soil layer. Such low-intensity events are expected to be more important at higher elevations, where strong convective storms are less common (Grimm et al.,

1995). A recent but preliminary examination of the Gross Reservoir Basin (South Boulder Creek) performed by Colorado Dam Safety suggests saturation-excess runoff might be important for extreme precipitation events (Perry et al., 2017). For the September 2013 storm that produced widespread flooding along the Colorado Front Range, the rainfall rate in the Gross Reservoir Basin never exceeded 3.1 cm/hr, but the storm continued for about six days. During that period, two peaks in rainfall intensity occurred approximately one day apart. Although the first peak had a higher rainfall intensity, the second peak produced much more runoff (Figure 1). This behavior is unexpected for infiltration-excess runoff, which would usually produce higher runoff rates for higher rainfall rates, but it is consistent with saturation-excess runoff, which depends more on the accumulated depth of rainfall.
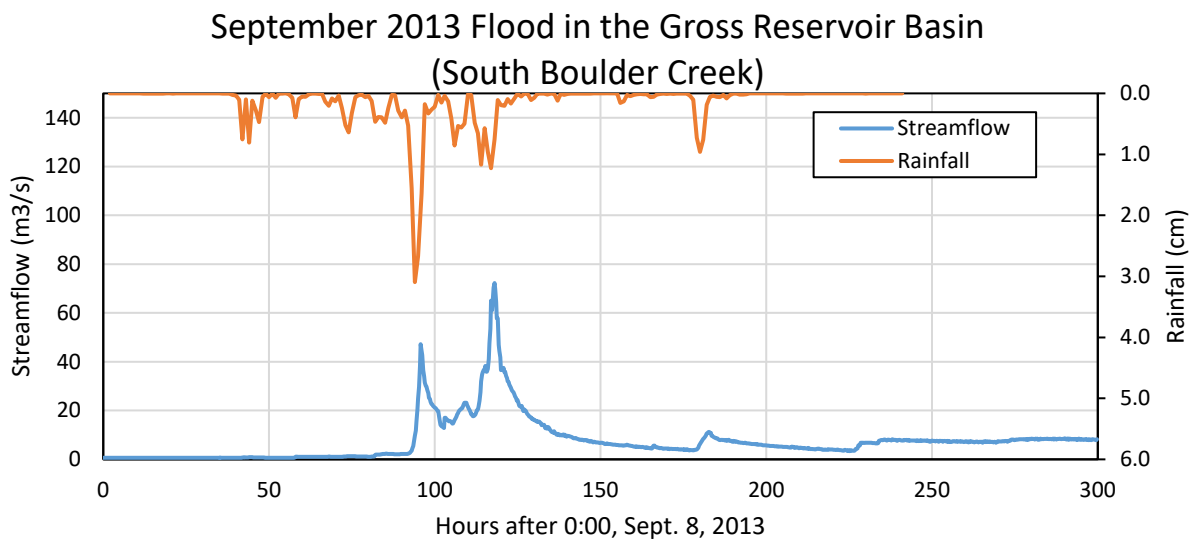
FIGURE 1. *Rainfall and streamflow observations from the September 2013 storm in the Gross Reservoir Basin (South Boulder Creek).*

Similarly, a study sponsored by the Colorado Department of Transportation (CDOT) calibrated a rainfall-runoff model to 10-day September 2013 flows in the upper Big Thompson River Basin and then used frequency rainfall estimates in the model to estimate frequency flows for bridge and culvert design. Their calibration efforts indicate high rainfall losses and almost no runoff until five days into the 10-day period, followed by a sudden change to minimal losses and high runoff (Jacobs, Inc., 2014). Although a physical explanation was not provided, these results are also consistent with saturation-excess runoff.

Finally, both the Colorado Dam Safety and CDOT studies had difficulty reproducing the observed hydrograph recessions for historic long-duration events in mountain basins. This problem appears to be associated with lateral subsurface flow (i.e., interflow) and may be consistent with a saturation-excess model where high volumes of water are temporarily stored in relatively coarse-grained shallow soils.

The overall objectives of this line of research are to determine whether the present Colorado Dam Safety guidelines for runoff modeling correctly specify the runoff production mechanisms for extreme precipitation events in Colorado's mountain basins and to develop updated guidelines for runoff modeling that include the appropriate runoff production mechanisms. The immediate goals for this first year of research are to:

(1) determine the runoff production mechanism that was active for the September 2013 floods based on available soil moisture data;

(2) develop a physically-based model that allows production of both infiltration-excess and saturation-excess runoff, and examine the mechanisms that were active for South Boulder Creek during the September 2013 event; and

(3) develop a foundation for extending this research to other storms and basins during the second year of this project (the second year is sponsored by the Mountain-Plains Consortium (MPC) with supplemental funding through a Federal Emergency Management Agency (FEMA) National Dam Safety Program (NDSP) grant obtained by Colorado Dam Safety).

The body of this report is organized according to these three goals. Section 2 presents the analysis of soil moisture observations. Section 3 describes the modeling of South Boulder Creek, and Section 4 describes the foundation that has been developed for other storms and basins. Although this document is a completion report for the Colorado Water Institute (CWI) and the CWCB project, the research is continuing under a second year of funding from the MPC. Thus, all results in this report should be considered interim results, and readers are encouraged to find finalized results in documentation at the end of the MPC project.

2. ANALYSIS OF SOIL MOISTURE OBSERVATIONS

Summary of Methods

In-situ observations of volumetric water content in the soil (i.e., soil moisture) are potentially valuable for identifying the runoff production mechanism that is active during extreme rainfall events like the September 2013 flood. For infiltration-excess runoff, high rainfall rates are expected to produce saturated conditions at the ground surface. The saturation limits the ability of the soil to infiltrate water and produces runoff. Because the soil at deeper levels might remain unsaturated when runoff is occurring, this runoff production mechanism is sometimes called "saturation from above." For saturation-excess runoff, prolonged rainfall is expected to produce saturated conditions first at the base of the soil layer (on top of the bedrock or other restrictive layer). As the storm continues, the saturated portion of the soil eventually reaches the ground surface at which point infiltration is limited and runoff occurs. This mechanism is sometimes called "saturation from below."

To evaluate the active runoff mechanism, soil moisture data from the 2013 flood were obtained from three sources: a research catchment in the Cache la Poudre River Basin (Traff et al., 2015), the National Climatic Data Center (NCDC) (Diamond et al., 2013; Bell et al., 2013), and the Boulder Creek Critical Zone Observatory (CZO) (Anderson et al., 2018). Figure 2a shows the approximate location of the Cache la Poudre research catchment. The catchment drains to the east and includes north-facing slopes (NFS) and south-facing slopes (SFS). The NFS are primarily forests comprised of Ponderosa pine and scattered Douglas fir, while the SFS are mainly shrubland with abundant mountain mahogany and antelope bitterbrush (Traff et al., 2015). Each hillslope was monitored with 22 Time Domain Reflectometry (TDR) sensors that measure soil moisture over 0-5 cm depth. Most probes were positioned under the canopy of the three dominant plant species in the catchment (Ponderosa pine, mountain mahogany, and antelope bitterbrush). Two additional probes were located in open areas. Precipitation was also measured at this catchment.

Figure 2b shows the approximate location of the NCDC soil moisture sensors. NCDC operates three co-located dielectric sensors at the site and provides an average soil moisture at 5 cm depth. This site is located on a SFS that is moderately forested.

Figure 2c shows the approximate locations of the soil moisture sensors from the Boulder Creek CZO. The Betasso site consists of two monitoring locations with three Decagon EC-5 soil moisture sensors. At one location, the measurement depths are 15 cm, 40 cm, and 70 cm. At the other location, the measurement depths are 40 cm, 70 cm, and 110 cm. The Betasso site is south-facing and primarily forested with Ponderosa pine. The sensors at the Lower Gordon Gulch site are aligned on a transect across the gulch with three locations on NFS, four locations on SFS, and one location immediately adjacent to the stream. Two locations utilize Decagon 5TE soil moisture sensors, while the remaining locations use Campbell Scientific CS616 sensors. The measurement depths vary among these sites but can include up to four measurement depths and range from 5 cm to 100 cm. The NFS are more densely forested than the SFS, which is common in the Colorado Front Range. Additionally, the mobile regolith is thicker on NFS than SFS, and the bedrock beneath the mobile regolith is weathered more significantly on the NFS (Anderson et al., 2013). Only one monitoring location is available at the Upper Gordon Gulch site with Campbell Scientific CS616 soil moisture sensors at four depths (5 cm, 50 cm, 100, cm, and 138 cm). The soil characteristics of the Upper Gordon Gulch site are similar to those of the Lower Gordon Gulch site. The site is slightly north-facing with dense vegetation.
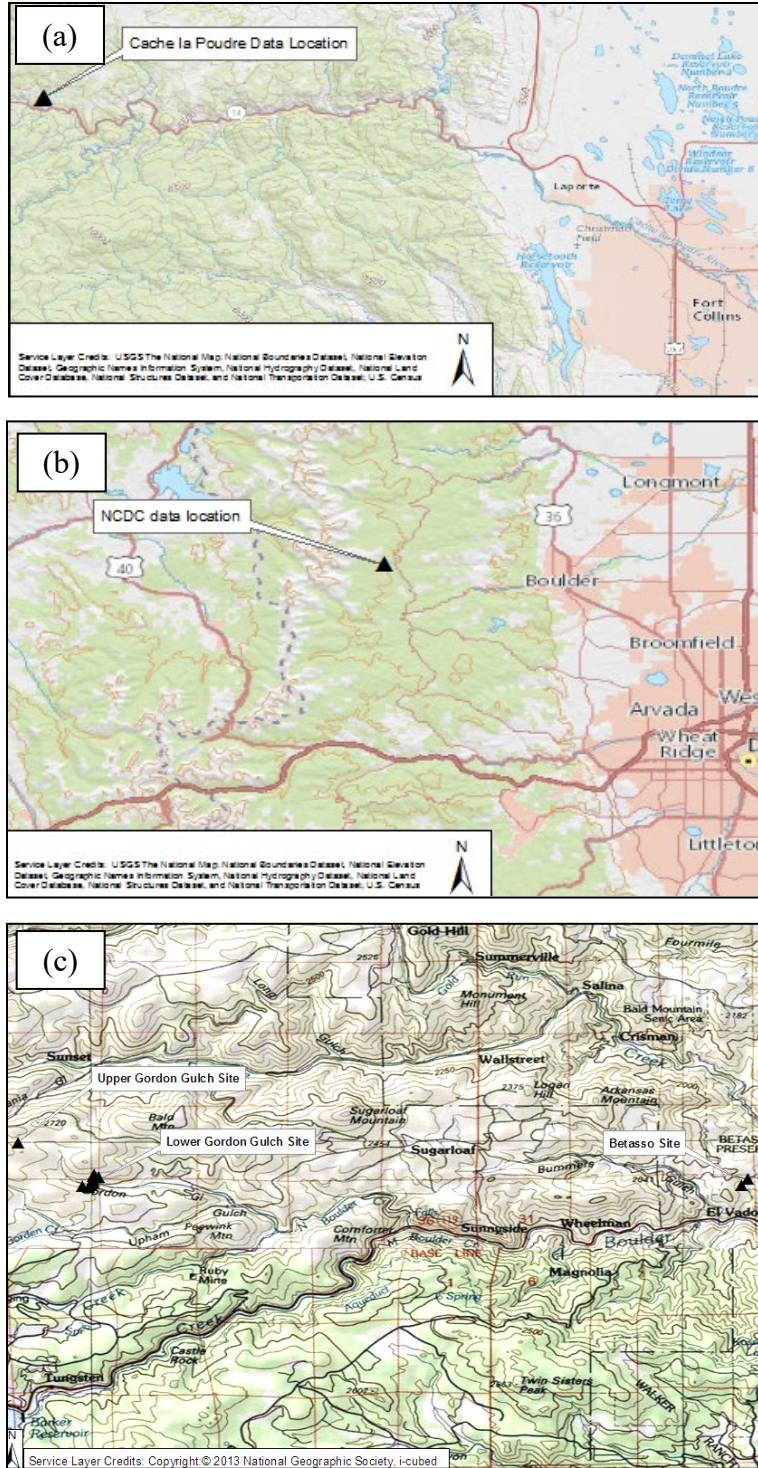
FIGURE 2. *Locations with available in-situ soil moisture observations including (a) the Cache la Poudre catchment, (b) the National Climate Data Center site, and (c) the Boulder Creek Critical Zone Observatory site.*

Discussion of Results

Figure 3a shows the soil moisture observations from an example location at the Cache la Poudre catchment. Saturation can be recognized by the constant high soil moisture value observed on 9/13/2013. Saturation occurs relatively late in the storm despite high rainfall rates being observed earlier in the event. This behavior may suggest that saturation occurred from below due to prolonged rainfall filling the soil. Unfortunately, multiple observation depths are not available at the Cache la Poudre site, so the cause of saturation is not conclusive.

Figure 3 also plots the soil moisture from three sites at the lower Gordon Gulch CZO area. At the flat site (Figure 3b), the periods with constant high soil moisture suggest that saturation is achieved at all levels of the soil column. Saturation begins first at the deepest layer and then progresses to shallower layers. This behavior supports the occurrence of saturation-excess runoff (saturation from below). The site on the SFS (Figure 3c) also clearly indicates prolonged saturation at the deeper layer (25 cm), and the very high soil moisture values at the shallow layer (5 cm) also may suggest brief saturation and runoff. This behavior is also consistent with saturation-excess runoff production. In contrast, the site on the NFS indicates runoff likely did not occur. The soil moisture is much lower than on the SFS, and it never reaches a high consistent value during the storm, indicating saturation did not occur at either depth. The behavior observed at these SFS and NFS is consistent with the other available sites. Of the 14 soil moisture measurement locations where it appears that saturation occurred during the 2013 storm, ten of the locations are on SFS. The observations of aspect-dependent saturation are consistent with the findings of Ebel et al. (2015), who also observed aspect-dependent saturation during the 2013 storm. They are also consistent with Coe et al. (2014), who found that 78% of the debris flows during the 2013 flood occurred on SFS. Saturated conditions on SFS would decrease the soil strength and promote instability and debris flows.
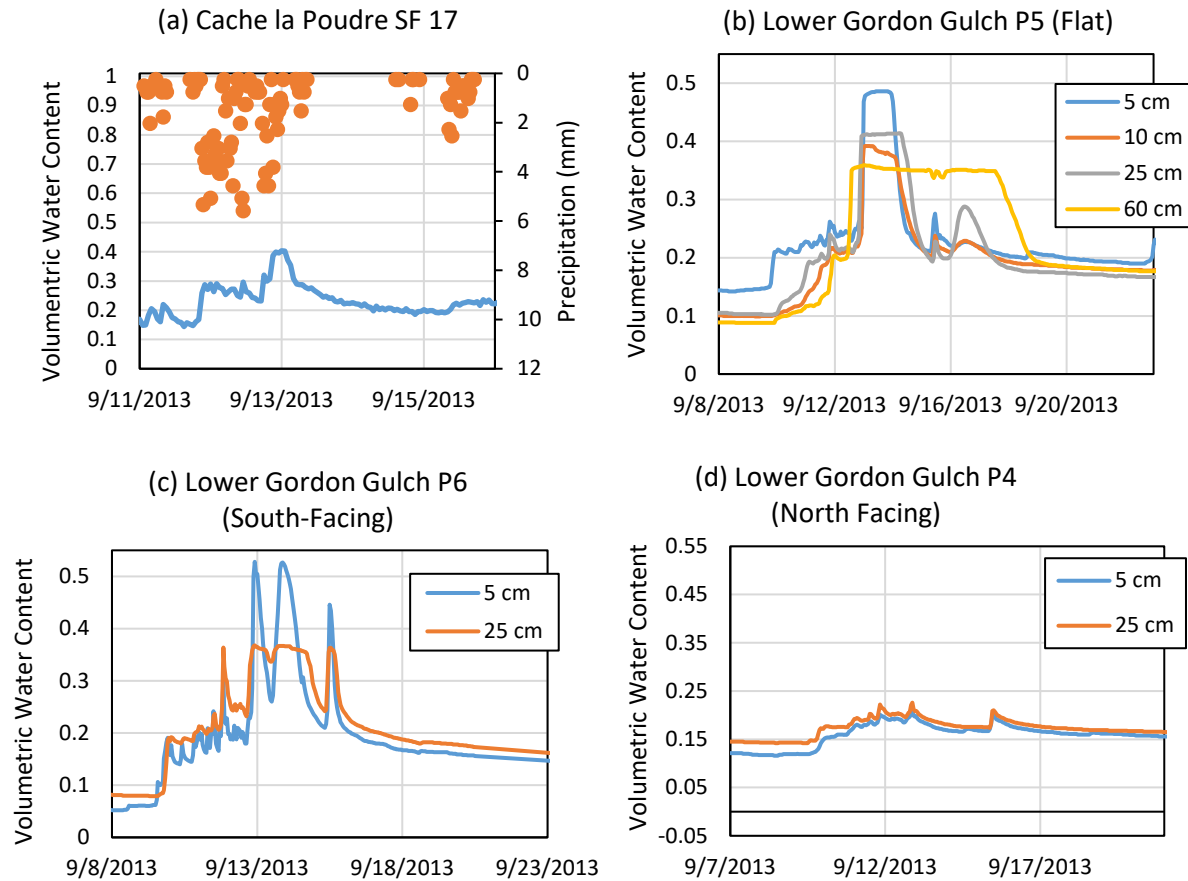
FIGURE 3. *In-situ soil moisture observations from various sites along the Front Range during the September 2013 flood.*

The preferential saturation on SFS is likely the result of a multiple factors. The most obvious difference between the NFS and SFS is the difference in vegetation density. Rengers et al. (2016) demonstrated that vegetation density is much higher on NFS. One effect of greater vegetation density is higher interception rates and lower throughfall rates. Reduced throughfall would inhibit soil saturation. Another effect of higher vegetation density is the formation of a connected drainage network in the bedrock. Bedrock can serve as an important water storage zone for woody vegetation in regions with thin, dry soils (Sternberg et al., 1996). Woody vegetation, such as Ponderosa pine, extends roots into the bedrock when moisture is unavailable in the soil layer (Witty et al., 2003). When dense forests persist in a region over a long period of time, this process creates fractures that serve as a connected drainage network.. The weathered drainage network is likely more extensive on densely forested NFS and leads to more rapid drainage of

soils and reduced possibility of saturation. An investigation of vegetation patterns in historical imagery shows that aspect-dependent forests have existed for at least the past 80 years (United States Forest Service, 1938).

3. SOUTH BOULDER CREEK MODEL

Summary of Methods

During the first year of this two-year project, a model was developed for the September 2013 flood for South Boulder Creek. This basin and storm event were used in part as a prototype for evaluating the key assumptions and modeling procedures that will be used for other basins during the second year. The model was implemented in the Hydrologic Engineering Center-Hydrologic Modeling System (HEC-HMS) (US Army Corps of Engineers, 2016). HEC-HMS was used because it is freely available and widely used by consultants for evaluating dam safety and reservoir operations. It also has a runoff modeling method called soil moisture accounting (SMA), which may be capable of adequately representing both infiltration-excess and saturation-excess runoff production.

Precipitation

Applied Weather Associates (AWA) used the Storm Precipitation Analysis System (SPAS) to quantify the spatial and temporal rainfall patterns for the September 2013 storm over the South Boulder Creek Basin. SPAS used observations from precipitation gauges to quantify rainfall amounts and relied on NEXRAD data to estimate the spatial distribution of precipitation between precipitation gauges (MetStat, 2018). AWA used observations from 2,635 stations throughout the Front Range to produce the SPAS results for the 2013 storm. Results were provided to the study authors in the form of gridded 60-minute rainfall depths (Figure 4).

Storm hyetographs were produced by calculating the spatial average within each sub-basin of South Boulder Creek for each 60-min precipitation grid using the ArcPy tool "Zonal Statistics as Table." Separate hyetographs were produced for NFS and SFS for each sub-basin within the watershed (see information about sub-basin determination below).
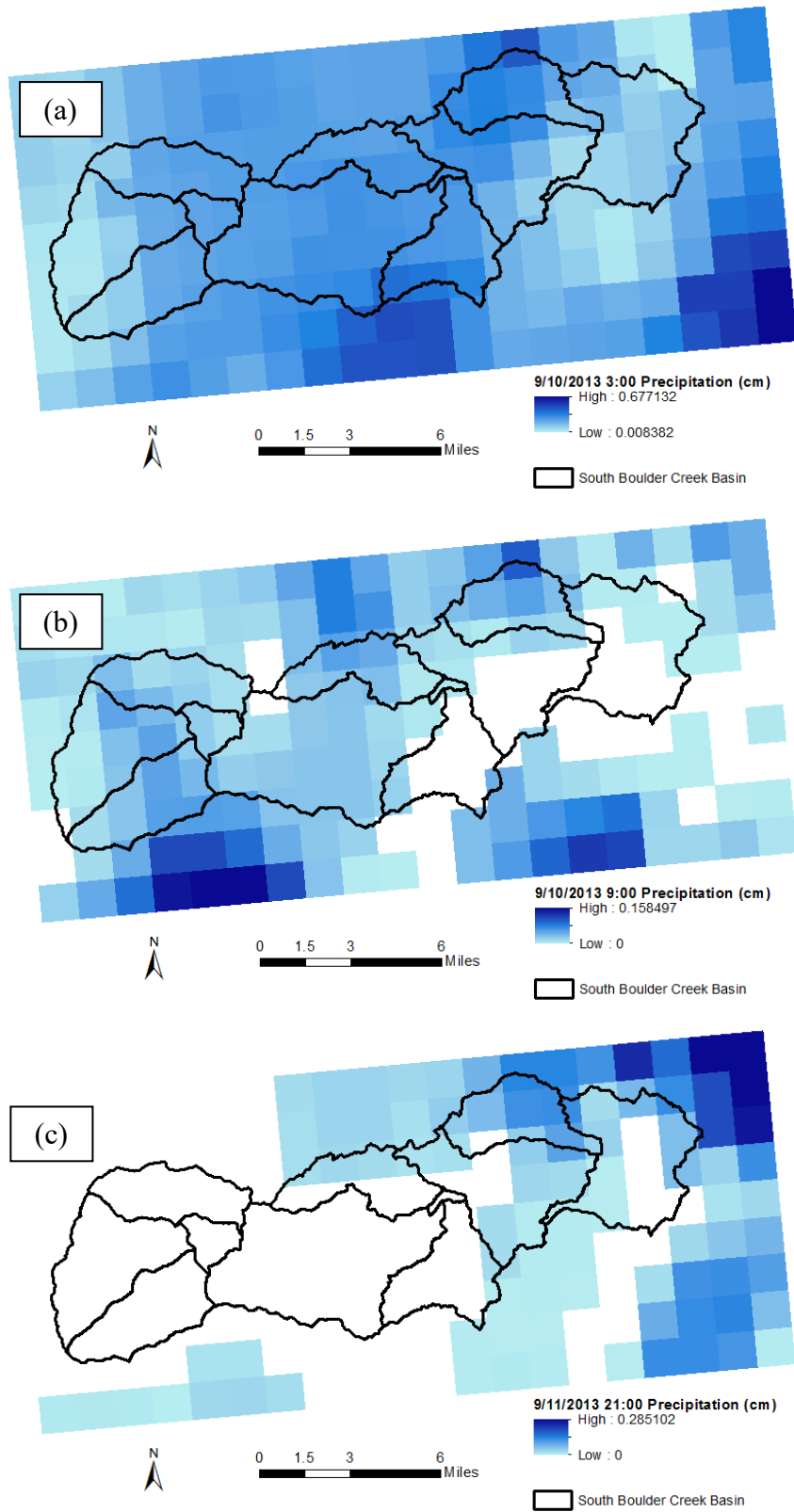
FIGURE 4. *60-minute precipitation depth grids for (a) 9/10/2013 3:00, (b) 9/10/2013 9:00, and (c) 9/11/2013 21:00.*

Sub-basin Disaggregation

The outlet location for the South Boulder Creek model was chosen to coincide with the Colorado DWR stream gauging station South Boulder Creek near Eldorado Springs (BOCELSCO) so that streamflow observations can used to calibrate and evaluate the model. South Boulder Creek's stage exceeded the gauge's existing rating curve during the 2013 storm, but DWR extrapolated the rating curve to estimate the discharge at the higher stages. The extrapolated curve was used in this study.

The South Boulder Creek Basin was disaggregated into sub-basins in order to better represent spatial variations of rainfall and watershed characteristics within the Basin. Within any given sub-basin, HEC-HMS considers very limited aspects of spatial variability, so the number of sub-basins is an important consideration in model development. Previous studies have shown that capturing the spatial variation of precipitation is the most important criteria in determining the level of basin disaggregation (Andreassian et al., 2004; Zhang et al., 2004).

ESRI's ArcHydro tools were used to delineate sub-basins using a 1/3 arc-second resolution digital elevation model (DEM) from United States Geological Survey's (USGS) National Elevation Dataset. Although a higher resolution LIDAR dataset is available for portions of some Front Range basins, it does not cover all of the basins that will be considered in this study (FEMA, 2013). The general procedure used for sub-basin delineation is as follows:

1. Fill sinks/pits in DEM to avoid undefined flow directions.
2. Determine flow direction of each DEM cell based on neighboring elevations.
3. Run flow accumulation tool to determine the number of cells flowing into each cell (i.e., the contributing area).
4. Create stream grid that indicates the presence/absence of a stream in each cell based on a selected contributing area threshold.
5. Separate stream grid into stream segments where confluences distinguish the segments.
6. Delineate a separate sub-basin for each stream segment.

The flow accumulation threshold described in Step 4 dictates the extent of the stream network and the implied number of sub-basins. A smaller contributing area threshold results in a more extensive stream network with more confluences and therefore more sub-basins. Because each sub-basin can accept a different record of precipitation, having more sub-basins typically improves the representation of precipitation variation in the basin model. Adequate disaggregation is achieved when the spatial variation within each sub-basin is relatively small. To evaluate different levels of basin disaggregation, the coefficient of variation (COV) of precipitation within each sub-basin was calculated for varying threshold areas. The objective is to identify a threshold area that reduces the average sub-basin COV as much as possible without producing unmanageable numbers of sub-basins.

This analysis was performed for several basins and extreme events in the Front Range because the identified threshold may depend on the basin and storm considered. In each case, threshold sizes from 4 km^2 to 35 km^2 were considered. Figure 5a plots the average sub-basin COV within the six study basins as a function of the selected contributing area threshold. For most basins, the average COV improves negligibly at the lower end of the threshold range, specifically below about 10 to 15 km^2. Figure 5b shows the number of sub-basins as a function of the contributing area threshold. The number of sub-basins increases substantially for some basins below 15 km^2 (even though the average COV decreases little). Thus, 15 km^2 was selected as the threshold that produces relatively homogeneous sub-basins while still maintaining a manageable number of sub-basins. Figure 6a shows the 11 sub-basins that were delineated for South Boulder Creek with the 15 km^2 accumulation area threshold.
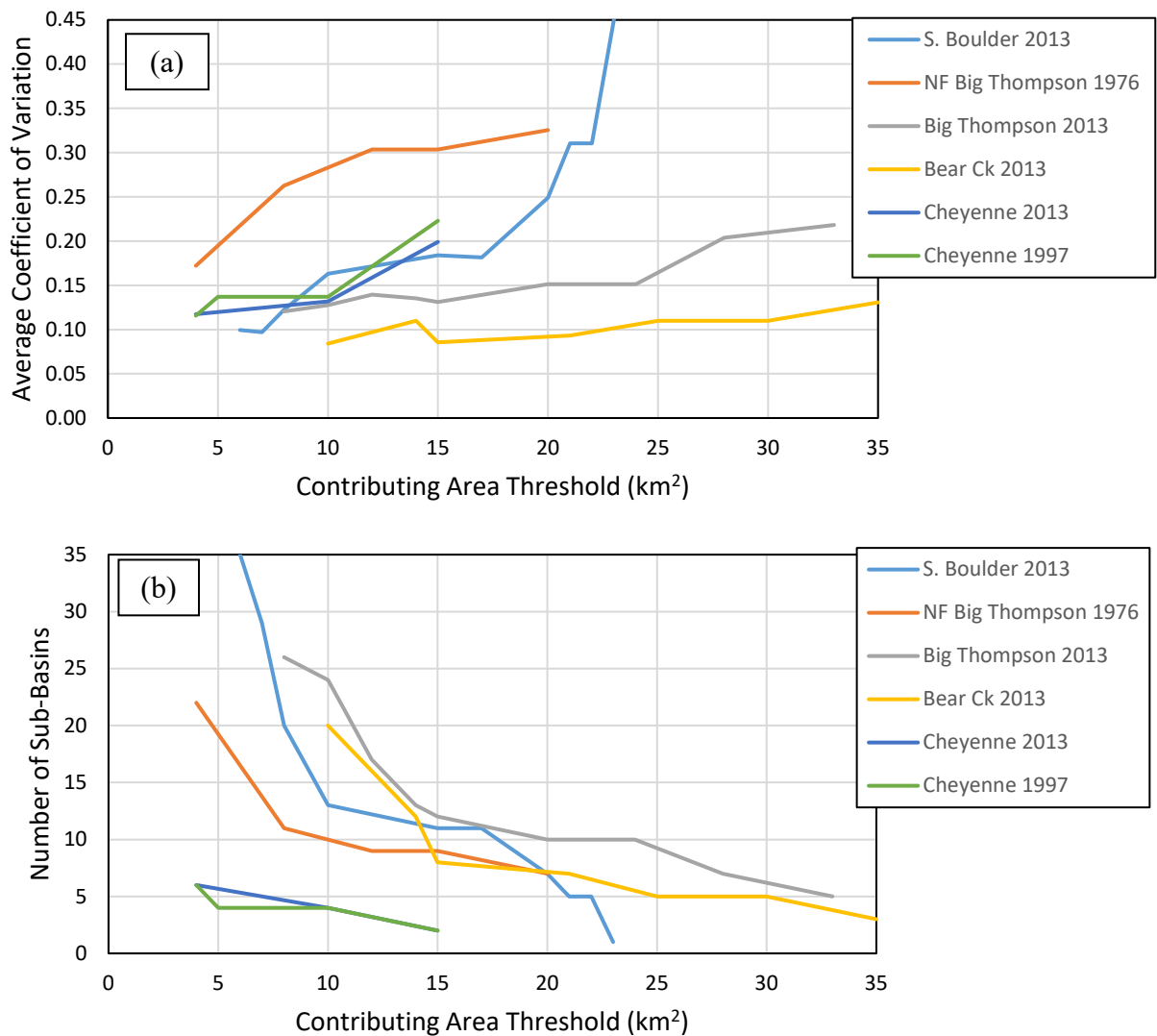
FIGURE 5. *(a) Average sub-basin coefficient of variation (COV) as a function of contributing area threshold and (b) number of sub-basins as a function of the contributing area threshold.*

Existing hydrology guidelines used by Colorado Dam Safety also state that sub-basins should be delineated so that they are reasonably homogeneous in terms of watershed characteristics (Sabol, 2008). Homogeneity is important because HEC-HMS uses uniform soil and vegetation characteristics within each sub-basin. As discussed earlier, NFS and SFS often have different vegetation cover, and their soil properties can differ as well. These physical differences also led

to the NFS and SFS behaving differently during the September 2013 storm as observed with the soil moisture data. Thus, it is potentially important to model NFS and SFS separately.

In the South Boulder Creek model, each sub-basin is divided into separate NFS and SFS elements. HEC-HMS models any sub-basin using unit hydrograph theory, which assumes a linear relationship between the sub-basin runoff and resulting stormflow and also implies additivity of stormflows (Sherman, 1932). Thus, the flows from the NFS and SFS can be summed to provide the total flows from a given sub-basin. This approach is very similar to the use of hydrologic response units, which is a common method used in other hydrologic modeling software (Flügel, 1995). Figure 6b shows the final HEC-HMS model elements implied by dividing the eleven sub-basins into their NFS and SFS.

Table 1 shows the average total storm precipitation depth in NFS and SFS parts of three basins analyzed during the 2013 storm. The results show SFS may have had slightly more precipitation, so the NFS and SFS in each sub-basin are provided separate precipitation hyetographs.

TABLE 1. *Average total storm precipitation for NFS and SFS*

	NFS Average Precipitation (cm)	SFS Average Precipitation (cm)
2013 Big Thompson River	15.7	15.7
2013 Bear Creek	17.8	19.1
2013 South Boulder Creek	18.5	19.3
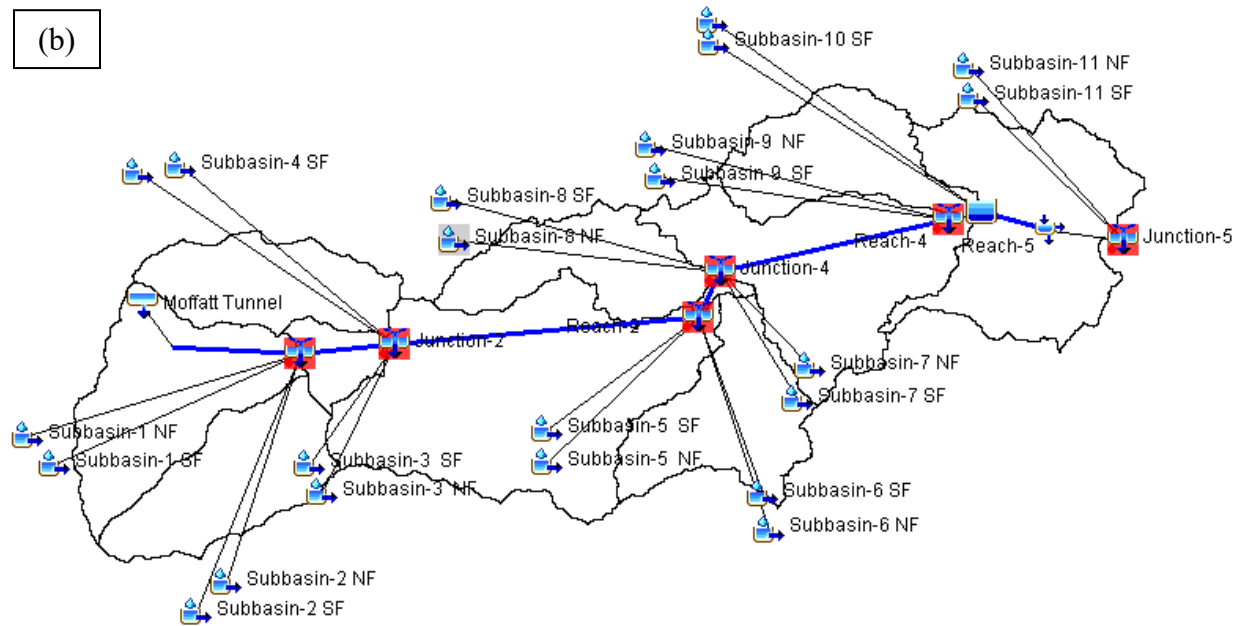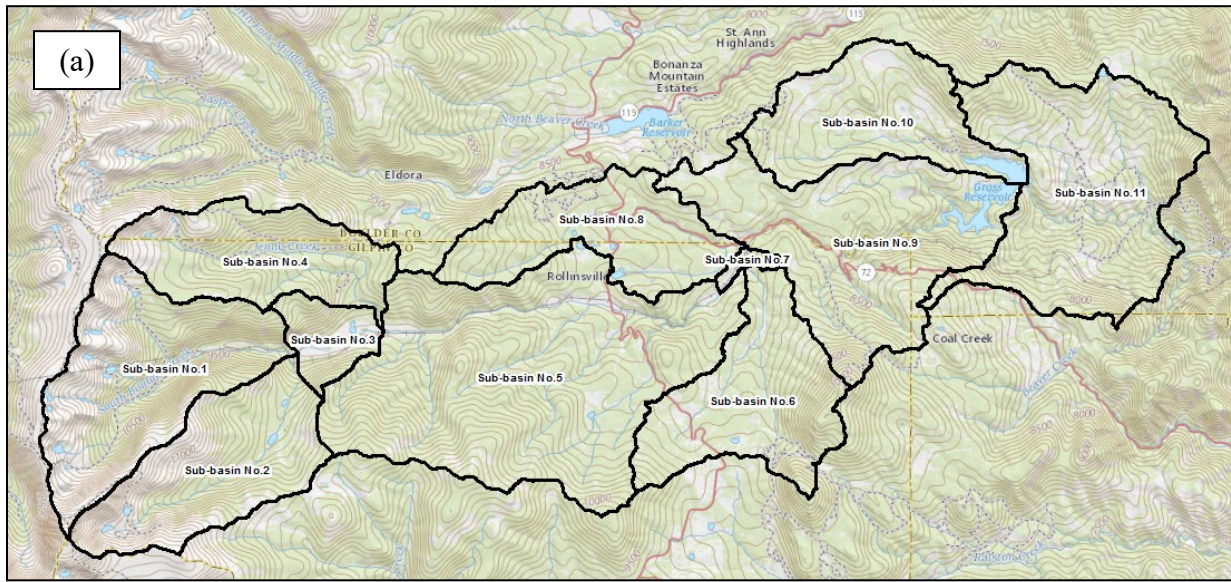
FIGURE 6. *(a) Map showing final sub-basins for South Boulder Creek, (b) HEC-HMS configuration of South Boulder Creek sub-basins.*

Loss Method

To achieve the project goals of determining and modeling the runoff mechanisms that are active for extreme rainfall events in the Colorado Front Range, the loss method used in this study must

allow simulation of both infiltration-excess and saturation-excess runoff. In addition, the model must not require calibration because many basins of interest are ungauged. The SMA loss method was chosen because it fulfills these requirements. Furthermore, SMA is the only loss method currently available in HEC-HMS that can simulate both infiltration-excess and saturation-excess runoff.

SMA defines the soil's infiltration capacity as a linear function of the current amount of water stored in the soil, as shown in Figure 7a. The linear function is defined by the maximum infiltration rate and maximum soil storage parameters. As Figure 7b shows, when the maximum soil storage nears infinity, the model produces a constant infiltration capacity irrespective of the soil storage. In this case, runoff only occurs when the rainfall rate exceeds the infiltration capacity, which similar to the existing guidelines for modeling runoff production that are used by Colorado Dam Safety (Sabol, 2008). It is also consistent with infiltration-excess runoff production. Alternatively, Figure 7c shows the case where the maximum infiltration rate nears infinity. In this case, all rainfall infiltrates until the soil is completely saturated (i.e., the soil storage reaches the maximum soil storage). At that point, all rainfall is runoff. This behavior is consistent with saturation-excess runoff.
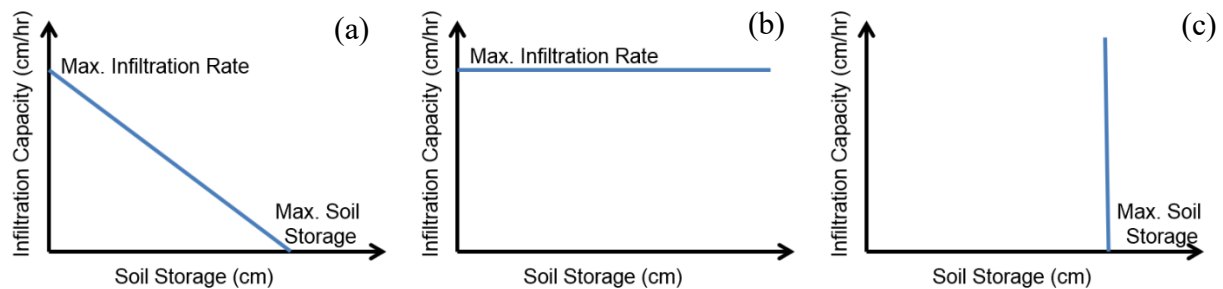
FIGURE 7. *(a) Infiltration capacity as a function of soil storage as represented by SMA, (b) SMA model produces infiltration-excess only as max soil storage goes to infinity, (c) SMA model produces saturation-excess only as max infiltration rate goes to infinity.*

Infiltration/runoff-production is only one part of SMA. Figure 8 shows a diagram of all components of SMA that are used in this study. Incoming rainfall first encounters the canopy storage, which simulates interception. All rainfall is captured by the canopy storage until it reaches its capacity (a parameter). After that point in time, all rainfall becomes throughfall.

Throughfall is then partitioned into infiltration and runoff using the linear infiltration function described earlier. Runoff is directed into the unit hydrograph component of the HEC-HMS model (described later) and ultimately becomes storm flow in the stream, while infiltrated water enters the soil storage. Water leaves the soil storage only as percolation to a groundwater layer (all evapotranspiration is neglected because the model will only be used to simulate individual events). This groundwater layer represents water that collects on top of the bedrock surface and ultimately produces interflow (sub-surface stormflow). Percolation between the soil and groundwater layers depends on the storage in both layers and a maximum percolation rate parameter. Water can exit the groundwater layer either as percolation to deeper groundwater (this water would ultimately become baseflow, but is considered lost because baseflow is not simulated) or as interflow. The deep percolation is a function of the simulated groundwater storage and a maximum deep percolation rate. Interflow is calculated using the assumption that the groundwater storage behaves as a linear reservoir. Thus, the groundwater's linear reservoir time constant is another parameter. From there, the interflow enters into a second linear reservoir (which requires a second time constant), after which it enters the stream and is combined with the stormflow produced by the runoff. While SMA has parameters that are not entirely physically-based, it can model all of the relevant processes. In addition, its parameters can be inferred from the physical characteristics of the basin.
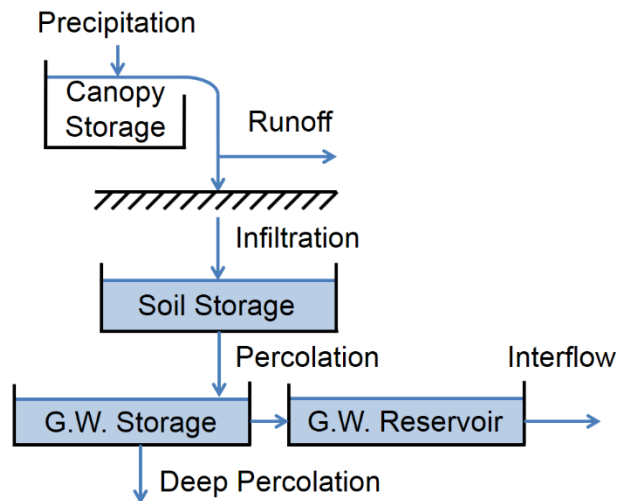
FIGURE 8. *Diagram illustrating the soil moisture accounting (SMA) model components.*

The SMA method includes parameters for the canopy storage, soil storage, groundwater storage, and groundwater reservoir. The canopy parameters are the initial canopy storage and the

maximum canopy storage. The soil parameters include the initial soil storage (as a fraction of the maximum soil storage), maximum infiltration rate, maximum soil storage, and maximum soil percolation. The groundwater parameters include the maximum groundwater storage, initial groundwater storage, two groundwater time coefficients, and the maximum deep percolation rate.

Canopy storage was based on rainfall measurements in the Cache la Poudre River catchment during the September 2013 storm (Traff et al., 2015). Three precipitation gauges were located on NFS and two were located on SFS. Two NFS gauges were located under tree canopy that was representative of the slope, while one was placed in the open. One SFS gauge was placed under the shrub canopy, while one was in the open. Canopy storage can be estimated as the difference between the precipitation measured in the open and that under the canopy. The interception rates were used to estimate the NFS and SFS interception rates in the model. During the second year of the project, additional research will be conducted on canopy interception in the Front Range to finalize the canopy storage values.

The soil layer parameters were estimated primarily using the Natural Resources Conservation Service (NRCS) Soil Survey Geographic (SSURGO) database. The dominant percent sand, percent clay, and percent organic matter layer in the top 45.7 cm were extracted from the SSURGO database. This depth was chosen based on Colorado's existing guidelines for storms that are less frequent than the 100-year event (Sabol, 2008). The soil characteristics were then supplied to pedotransfer functions (Saxton and Rawls, 2006; Rawls et al., 1983), which calculate the bare ground saturated hydraulic conductivity K_{sat}, porosity ϕ, field capacity θ_{fld}, wilting point θ_{wp}, and wetting front suction head ψ_f. K_{sat} was then adjusted for vegetation cover based on existing hydrology guidelines for Colorado (Sabol, 2008). This adjustment increases the K_{sat} values for thickly vegetated areas. The maximum infiltration rate was then calculated based on the Green-Ampt infiltration model (Green and Ampt, 1911), which states:

$$f = K_{sat}\left[1 + \frac{|\psi_f|(\phi - \theta_i)}{F}\right]$$

where f is the infiltration capacity, θ_i is the initial soil moisture, and F is the cumulative infiltration for the time when f is being calculated. To calculate the maximum infiltration

capacity parameter, the Green-Ampt infiltration capacity was calculated when the wetting front reaches a selected depth δ. At this point in time:

$$f = K_{sat}\left[1+\frac{|\psi_f|(\phi-\theta_i)}{\delta(\phi-\theta_i)}\right] = K_{sat}\left[1+\frac{|\psi_f|}{\delta}\right]$$

The depth was chosen to be 22.9 cm, which is half of the depth used to determine the soil characteristics according to the existing Colorado hydrology guidelines. The selected depth will be examined in more detail in the second year of the project.

The maximum soil storage is estimated using the depth to restrictive layer from the SSURGO database. Specifically, the maximum soil storage is calculated as:

$$S_{max} = Z\phi$$

where S_{max} is the maximum soil layer storage and Z is the depth to restrictive layer.

According to Colorado's existing hydrology guidelines, the fractional initial soil storage should be estimated based on the assumption of either dry or normal conditions preceding the event. Dry conditions occur when the soil moisture is near the wilting point, while normal conditions occur when it is near the field capacity. Soil moisture estimates from the North American Land Data Assimilation System (NLDAS) were used to determine that the conditions preceding the September 2013 event were normal (Xia et al., 2012; NCEP/EMC, 2009). Based on this determination, the initial soil storage percent was calculated using the field capacity:

$$Fs_{init} = \frac{Z\theta_{fld}}{S_{max}}$$

The maximum percolation rate was estimated from the Colorado Geologic Map, which was obtained from Colorado Geological Survey and the USGS National Geologic Map Database (Kellogg, et al., 2008). The primary rock type at a given location was selected to characterize the bedrock, and the lower bound of the associated hydraulic conductivity from Domenico and Schwartz (1990) was used as the maximum percolation rate.

The groundwater parameters were estimated based on an analysis of the 2013 storm hydrograph recession (Fleming and Neary, 2004; Linsley et al., 1958). It is assumed that the hydrograph

recession is produced by interflow and baseflow, and that both processes behave as linear reservoirs. Under these assumptions, the contribution of the baseflow to the recession can be determined and removed. Furthermore, the interflow as a function of time is expected to follow an exponential equation. After the baseflow has been removed, an exponential equation can be fit to the interflow, and the time constant of the exponential equation is related to the overall time constant for the groundwater. When SMA is used, the interflow is actually produced by two linear reservoirs in sequence. Thus, the time constant for each reservoir was chosen to be half of the time constant obtained from the hydrograph analysis. These values were then manually calibrated, and the calibrated values range from 2-5 hr. The exponential equation can also be used to estimate the maximum groundwater storage that occurred during the storm. While this is not the maximum capacity of the groundwater layer, it is used to estimate the maximum groundwater layer storage. The maximum capacity is initially set equal to the maximum storage during the storm, then it is manually calibrated. The final calibrated values range from 1.2-3 mm. The maximum deep percolation rate is initially set to 0 mm/hr, then it is manually calibrated. Currently, calibrated values are in the range of 0-3 mm/hr. All of these approaches will be examined in more detail in the second year of the project.

<u>Direct Flow Transform</u>

Runoff produced by SMA is transformed into stormflow at each sub-basin outlet using Clark's unit hydrograph method (Clark, 1945). Clark's method was selected because it is among the methods recommended in the existing guidelines used by Colorado Dam Safety and because it has the capability to include the distinction of NFS and SFS. Clark's method uses a cumulative time-area curve, which describes the distribution of travel times from each point in a sub-basin to the sub-basin outlet. This curve is used to determine a unit hydrograph for the sub-basin. When the unit hydrograph is used, the resulting outflow is then routed through a linear reservoir to account for flow storage and hydrograph attenuation. The cumulative time-area curve can be provided by the modeler to HEC-HMS. A user-defined curve is useful in our situation because NFS and SFS are modelled separately. Thus, separate time-area curves need to be developed for the NFS and SFS points in each sub-basin.

A model was written in ArcPy to calculate the cumulative time-area curve and will be used to simulate additional storms and basins in the Front Range for the second year of the study. The general procedure used is as follows:

1. Use the ArcGIS Slope tool to calculate the slope of each cell in the basin.

2. For channel cells, calculate the travel time per cell t using Manning's equation: $t = dn \left[\frac{1}{R^{2/3} S^{1/2}} \right]$ where d is the cell length, R is the hydraulic radius, S is the slope, and n is Manning's roughness coefficient. The hydraulic radius is calculated assuming a rectangular channel and using relationships that relate both bankfull width and depth to contributing area for the Colorado Front Range (Livers and Wohl, 2015). Manning's roughness is determined based on representative values for land cover types (Chow, 1959) and land cover data from the National Land Cover Dataset 2011.

3. For hillslope cells, calculate travel time per cell t using a Manning's equation approximation: $t = \frac{d}{k S^{1/2}}$ where k is a coefficient that includes both the roughness and hydraulic radius. A constant k was used for the entire basin, and the value was selected to produce realistic overland flow velocities (which can be inferred from the travel time equation). Average overland velocities range from 0.17-0.27 m/s, while average channel velocities range from 0.79-2.45 m/s.

4. Calculate the total travel time from each cell to the basin outlet and develop cumulative distribution of these times (which is the time-area curve).

Figure 9 shows examples of the time-area curves developed for South Boulder Creek sub-basins.
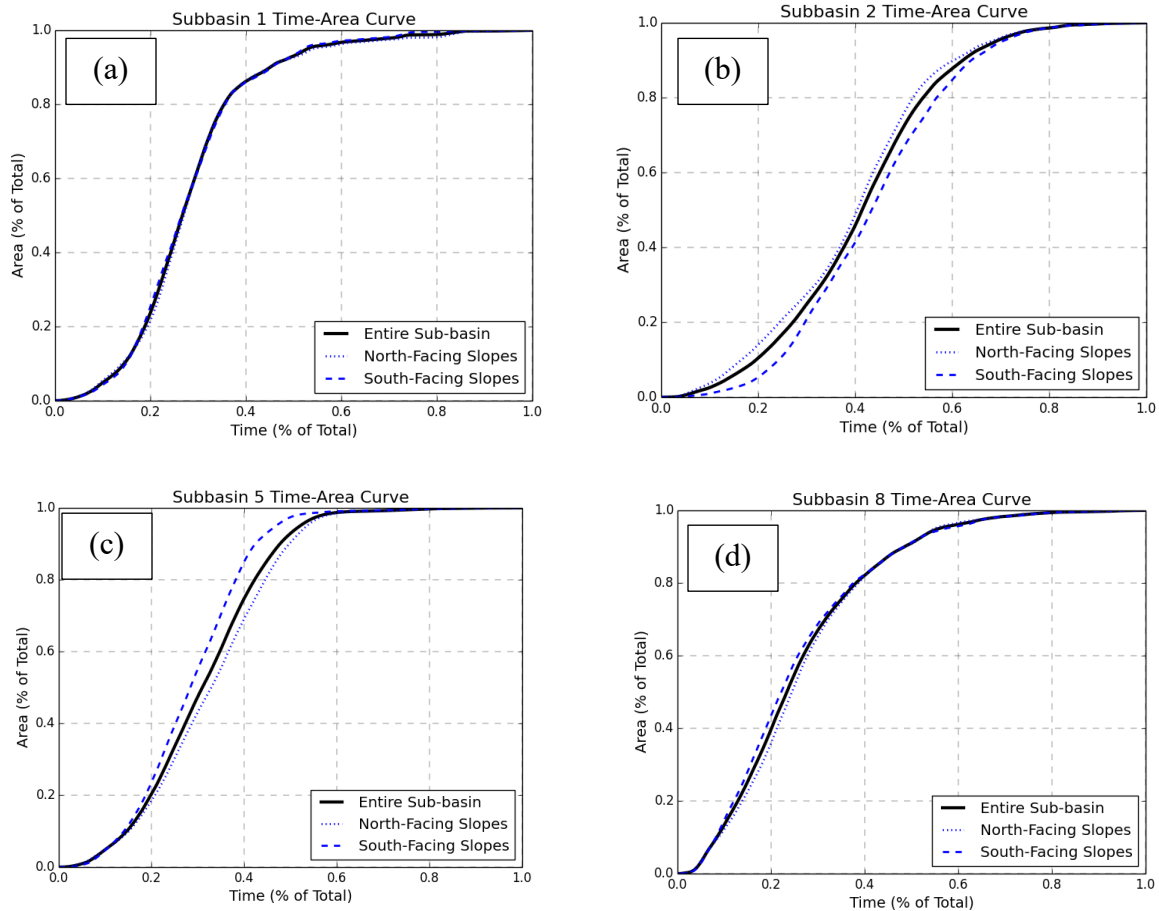
FIGURE 9. *Time-area curves developed for sub-basins 1, 2, 5, and 8, respectively.*

In addition to the time-area curve, the Clark method also requires the time of concentration T_c for each sub-basin and the storage coefficient R for each sub-basin's linear reservoir. The existing guidelines used by Colorado Dam Safety produce times of concentration that are much shorter than those calculated from the method used to calculate the time-area curves. Furthermore, the velocities implied by the existing guidelines are higher than expected. Thus, the maximum time for each sub-basin's accumulated travel time raster was used as its time of concentration. To obtain the storage coefficient, both the time of concentration and storage coefficient were calculated using the existing Colorado hydrology guidelines. Then, the ratio of the two values was used to calculate the storage coefficient that corresponds to the time-area method's time of concentration.

Channel Routing

The method "Muskingum-Cunge with Eight Point Cross-Sections" was used to route streamflow through channel reaches in the basin model. This method was selected because it is the only currently available method that allows flow to occur outside of the channel (on the floodplain) aside from Modified Puls, which cannot be used without calibration (Feldman, 2000). The Muskingum-Cunge method is applicable for a wide range of channel slopes and flow depths. It also accounts for both the lag and attenuation of the hydrograph as it moves through the reach.

The Muskingum-Cunge method requires the coordinates of eight points to define the channel and floodplain cross-section geometry. It also requires specification of a roughness coefficient. The channel width was measured using aerial imagery, and the depth was calculated iteratively using Manning's equation assuming bankfull flow. Representative floodplain dimensions were estimated manually from the valley geometry as described by the DEM. Roughness coefficients were estimated from channel type and floodplain vegetation based on aerial imagery and representative roughness values (Chow, 1959).

Reservoir Routing

Gross Reservoir is embedded in the South Boulder Creek basin and must be modeled. HEC-HMS always uses a version of Modified Puls (or Storage-Indication) routing for reservoirs, but the user can specify the required storage-discharge relationship in a variety of ways. For the South Boulder Creek model, an elevation-storage curve, specifications of the reservoir's outlet structures, and an initial condition were provided. The reservoir elevation calculated at each time step from the elevation-storage curve is used to calculate the reservoir's outflow based on the outlet structure information. All of the inputs to the routing method were taken from information provided by DWR and Denver Water, who owns and operates Gross Reservoir.

Diversions

There are two diversions in the South Boulder Creek Basin. The Moffat Tunnel diverts water from the Colorado River Basin across the Continental Divide into South Boulder Creek. Its outlet is located toward the headwaters of the South Boulder Creek Basin. The South Boulder

Creek Diversion Canal diverts water out of South Boulder Creek Basin. This diversion is located upstream of Eldorado Springs. Flow data for both diversions were provided by DWR for the modeling period and used in the model.

Table 2 summaries the key parameters for all sub-basins in the South Boulder Creek model. These parameter indicate small differences between the NFS and SFS in each sub-basin and more substantial differences between the different sub-basins in the model. As discussed previously, the only values in Table 2 that were calibrated are the groundwater maximum storage, groundwater percolation, and linear reservoir coefficients.

TABLE 2. *Summary of the main model parameters for South Boulder Creek*

Subbasin	Aspect	Canopy Storage (mm)	Max. Soil Storage (cm)	Init. Soil Storage %	Max. Soil Infiltration (mm/hr)	Soil Percolation (mm/hr)	G.W. Storage (mm)	Sum of G.W. Linear Reservoir Coefficients (hr)	Clark U.H. T_c (hr)	Clark U.H. R (hr)
1	North	60	31.76	49%	62.62	0.562	1.2	7.9	6.4	2.3
1	South	25	28.16	50%	68.16	2.695	1.2	7.9	6.4	2.2
2	South	25	30.55	48%	63.40	3.394	1.2	7.9	4.6	2.1
2	North	60	28.31	50%	67.65	1.428	1.2	7.9	4.6	2.1
3	South	25	37.27	55%	59.47	7.947	1.2	7.9	7.2	2.4
3	North	60	41.58	57%	59.25	2.955	1.2	7.9	7.0	2.3
4	South	25	23.67	52%	69.67	5.703	1.2	7.9	5.6	2.7
4	North	60	27.22	53%	77.36	3.359	1.2	7.9	5.7	2.7
5	South	25	26.45	46%	66.66	2.053	1.2	7.9	6.1	1.5
5	North	60	25.43	47%	73.19	2.895	1.2	7.9	6.1	1.5
6	South	25	22.66	38%	90.38	9.956	1.2	7.9	5.2	1.9
6	North	60	21.78	36%	101.37	9.638	1.2	7.9	5.1	1.9
7	South	25	21.49	45%	52.22	11.880	1.2	7.9	4.4	3.0
7	North	60	23.92	46%	60.72	11.880	1.2	7.9	4.3	2.9
8	South	25	30.09	43%	64.48	21.294	1.2	7.9	6.2	1.7
8	North	60	27.37	45%	71.29	15.131	1.2	7.9	6.2	1.7
9	South	25	20.07	40%	60.73	38.536	1.2	7.9	7.9	3.4
9	North	60	22.83	38%	76.75	51.647	1.2	7.9	7.9	3.4
10	South	25	22.21	47%	56.13	39.441	1.2	7.9	4.9	2.1
10	North	60	22.90	40%	73.11	167.550	1.2	7.9	5.0	2.1
11	South	25	9.89	33%	82.03	11.868	1.2	7.9	4.6	1.3
11	North		12.66	37%	81.97	11.872	1.2	7.9	4.5	1.3

Table 3 shows the maximum infiltration rate used in Colorado's existing hydrology guidelines (Sabol, 2008). The existing guidelines do not account for the effect of the wetting front suction head on the infiltration rate as the proposed method does; therefore, the proposed rates are significantly higher. The values in Table 3 do not include the adjustment for vegetation used by the existing guidelines, so the values reflect the bare ground saturated hydraulic conductivity.

TABLE 3. *Maximum infiltration rate by USDA Soil Classification from existing Colorado hydrology guidelines (Sabol, 2008)*

USDA Soil Classification	Maximum Infiltration Rate (mm/hr)
Sand	116.84
Loamy sand & sand	30.48
Sandy loam	10.16
Loam	6.35
Silty loam	3.81
Silt	2.54
Sandy clay loam	1.524
Clay loam	1.016
Silty clay loam	1.016
Sandy clay	0.508
Silty clay	0.508
Clay	0.254

Discussion of Results

Figure 10 shows the preliminary results of the South Boulder Creek model at BOCELSCO (i.e., the basin outlet) for the September 2013 storm. These preliminary results may change during the second year of the project as the modeling methods continue to develop. The model reproduces the relative magnitudes of the two peaks of the hydrograph. Like the observations, the second peak in the model results is higher than the first peak. The model also produces hydrograph recessions that are similar to the observed recessions. The Nash-Sutcliffe Coefficient of Efficiency (NSCE) was used to quantify the model performance. An NSCE value of one would indicate the model perfectly matches the observations. An NSCE value of zero would mean the model matches the observations with the same accuracy as a model that is simply the mean of the observations (NSCE can also be negative). The NSCE for the South Boulder Creek model is 0.80, which suggests generally good performance. Mean Bias Error (MBE) was also used to

evaluate the model. A MBE value of zero would indicate the model is equally likely to overestimate and underestimate the flow at any point in time. A positive value of MBE indicates the model typically overestimates the flow. For the South Boulder Creek model, the MBE is 1.31 m^3/s. Overall, these results suggest that the model describes the key features of the observed hydrograph. In addition, because little calibration was performed to achieve these results, it suggested that uncalibrated models developed based on the approach described above have the potential to provide reasonable estimates of basin response when calibration is not possible.
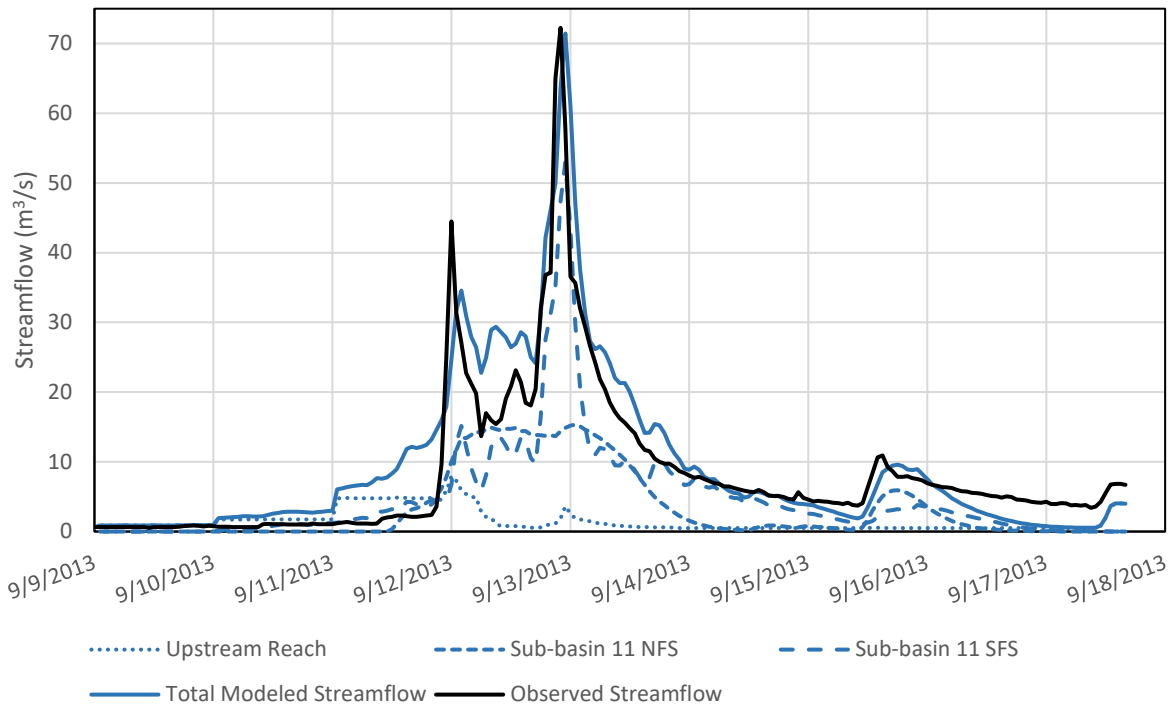

FIGURE 10. *Comparison of modeled streamflow and observed streamflow at the BOCELSCO stream gauge location (i.e., the outlet of the South Boulder Creek Basin). Blue lines indicate the total modeled streamflow and the contributions from the incoming model elements. Black line indicates the observed streamflow.*

Figure 10 also shows the contribution of flow from each model element that is connected to the outlet. The figure indicates that during the 2013 storm, Gross Reservoir (which supplies the upstream reach element) contained nearly all its incoming flow. Other than a small scheduled release from the reservoir, all modeled streamflow at the basin outlet is produced downstream of the reservoir (from sub-basin 11).

Figure 11 shows the streamflow produced by the NFS and SFS parts of sub-basin 11. All discharge generated from the NFS of sub-basin 11 is produced by interflow (Figure 11a). No surface runoff is produced from these areas. In contrast, discharge from the SFS includes both interflow and surface runoff (Figure 11b). While interflow produces most of the hydrograph for the SFS, the hydrograph peaks are largely produced by surface runoff.

Figure 12 shows the degree of saturation for the NFS and SFS of sub-basin 11. The soil storage for the NFS never approaches saturation, while the soil storage for the SFS does approach saturation during the period when the runoff is produced in Figure 11. These results are consistent with the available soil moisture observations, which show saturation often occurring on SFS but rarely occurring on NFS. It is interesting that complete saturation is not required for runoff production to occur in the model. When the soil storage approaches saturation, the infiltration capacity approaches zero. This low infiltration capacity is sufficient to produce runoff for the rainfall intensities that occurred during the event. Categorization of this runoff mechanism is difficult. One might consider it infiltration-excess because the soil is not completely saturated. However, the infiltration capacity is low because of the soil's limited storage capacity and the near saturation of the soil layer. Thus, one might consider it saturation-excess.

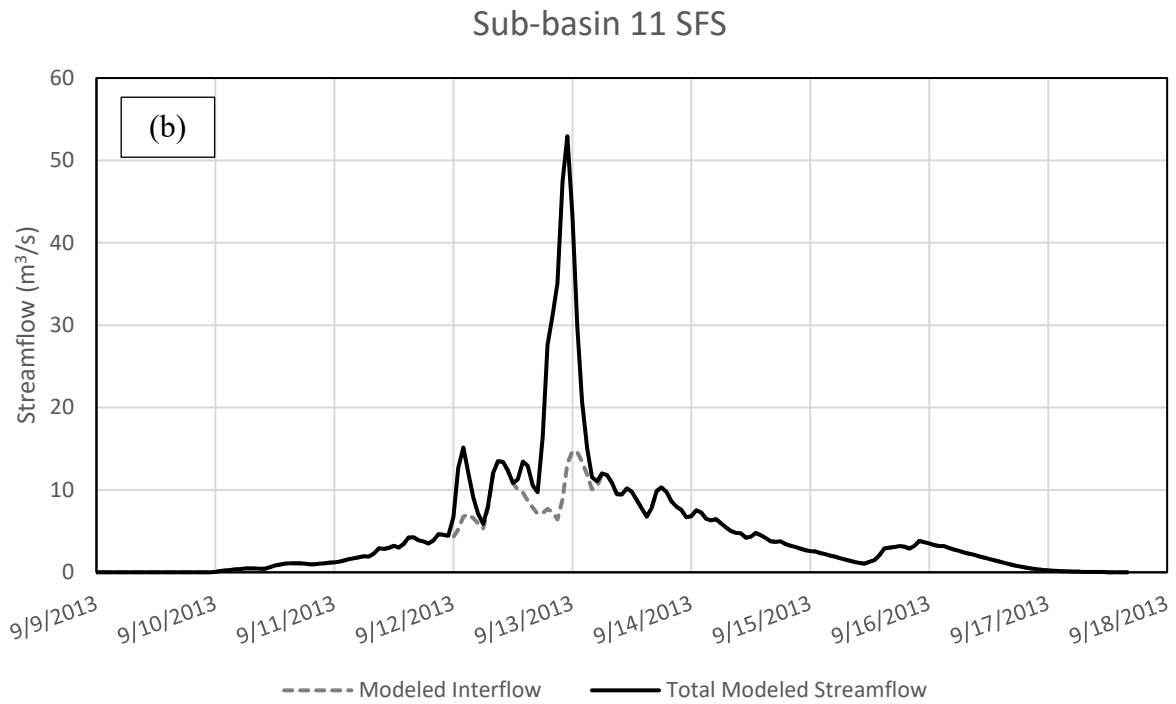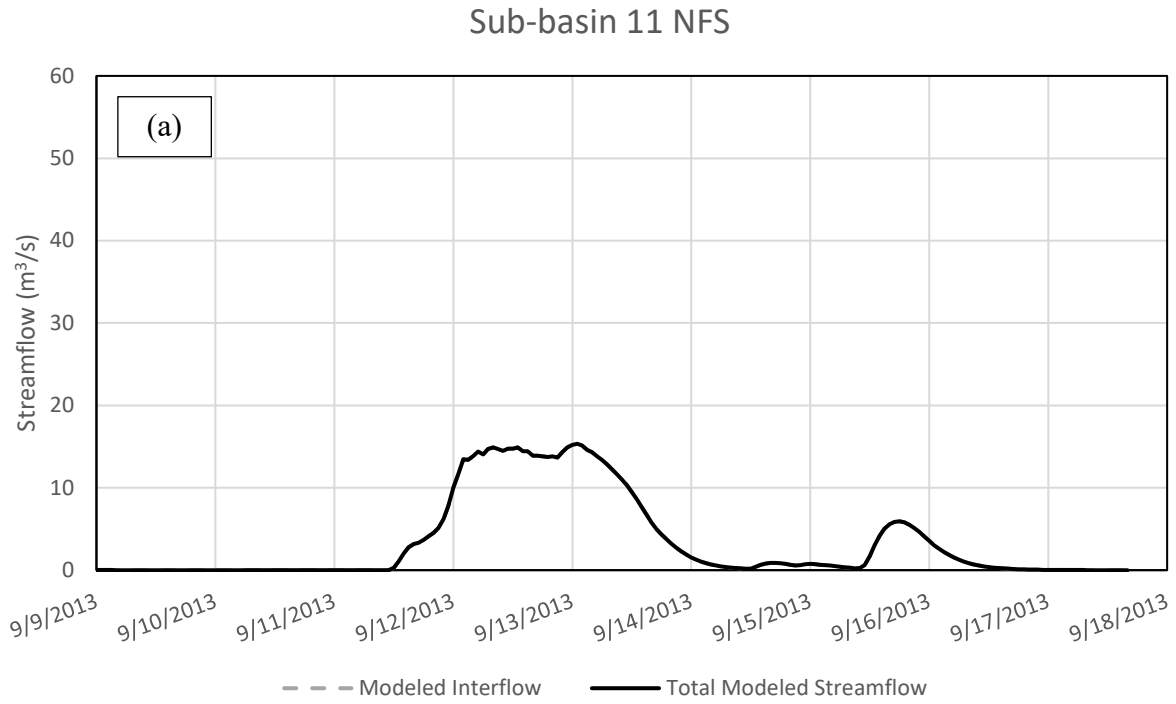## Sub-basin 11 NFS

(a)

Sub-basin 11 SFS

(b)

FIGURE 11. *Modeled discharge produced by (a) sub-basin 11 north-facing slopes and (b) sub-basin 11 south-facing slopes.*
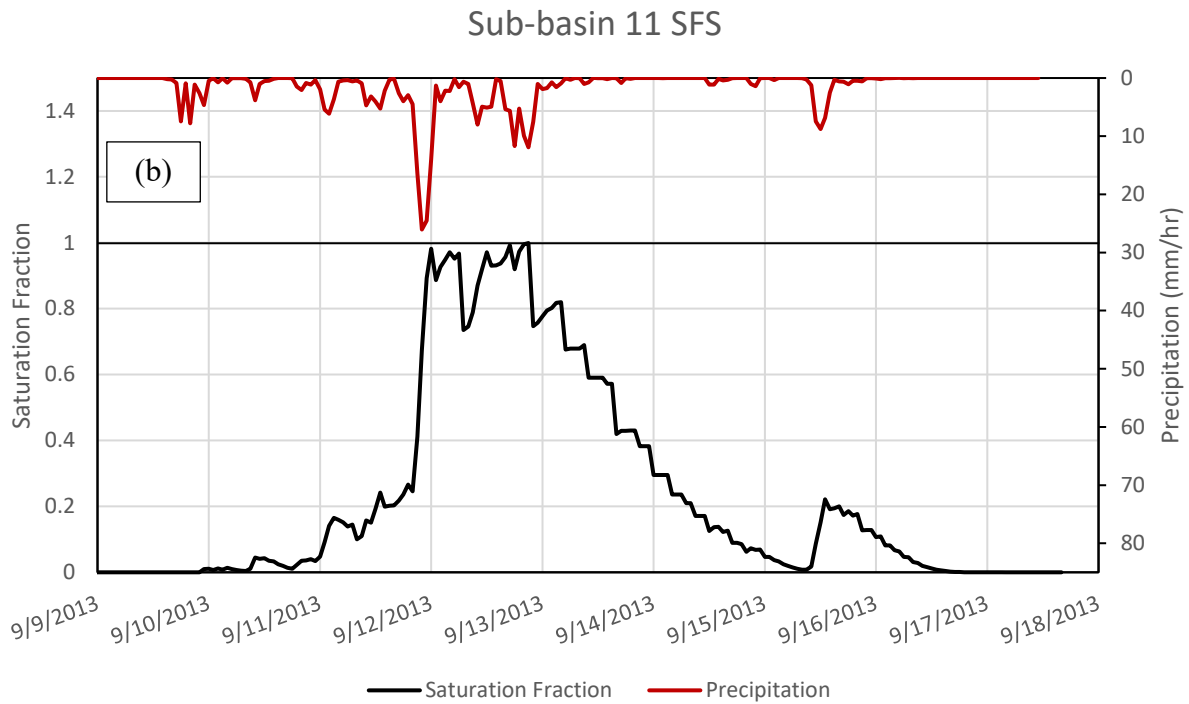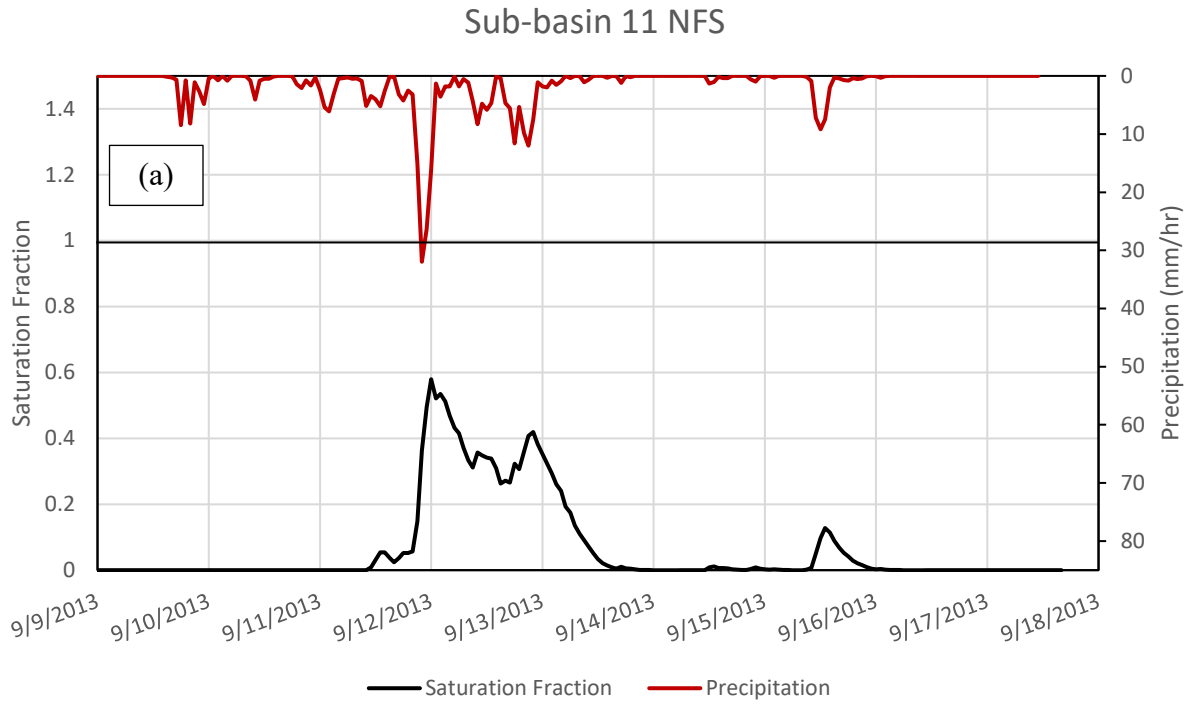
FIGURE 12. *Degree of saturation in the model for (a) sub-basin 11 north-facing slopes and (b) sub-basin 11 south-facing slopes.*

To further investigate the runoff production mechanism in the basin model, Figure 13 shows the results when the model has been forced to emphasize infiltration-excess runoff by setting the maximum soil storage to the largest allowable value in HEC-HMS (1500 mm). Figure 13 shows that the contribution from Gross Reservoir remains unchanged (it is the scheduled release). The hydrograph shape changes because the large soil storage reduces the interflow to the river. Most importantly, the model misses the hydrograph peaks because the soil never approaches saturation and the infiltration capacity remains high. Thus, runoff does not occur. This case is similar to the existing guidelines used by Colorado Dam Safety, which neglect the soil's limited storage capacity. However, the existing guidelines specify a lower maximum infiltration capacity than the value used here because they neglect the contribution the pressure gradient in determining the infiltration capacity (i.e., ψ_f). Thus, a model based on those guidelines might produce infiltration-excess runoff.

FIGURE 13. *Comparison of modeled streamflow and observed streamflow at the BOCELSCO stream gauge location when the model is forced to emphasize infiltration-excess runoff.*

Figure 14 shows the model results for a case where the model has been forced to emphasize saturation-excess runoff. This case is produced by setting the maximum infiltration capacity to the largest allowable value in HEC-HMS (500 mm/hr). Overall, the results remain very similar to

the original calibrated model (Figure 10). Together, the cases shown in Figures 12 and 13 confirm that the runoff production in the original (Figure 10) model occurs due to the soil's limited storage capacity. They also suggest the generated runoff is best classified as saturation-excess.
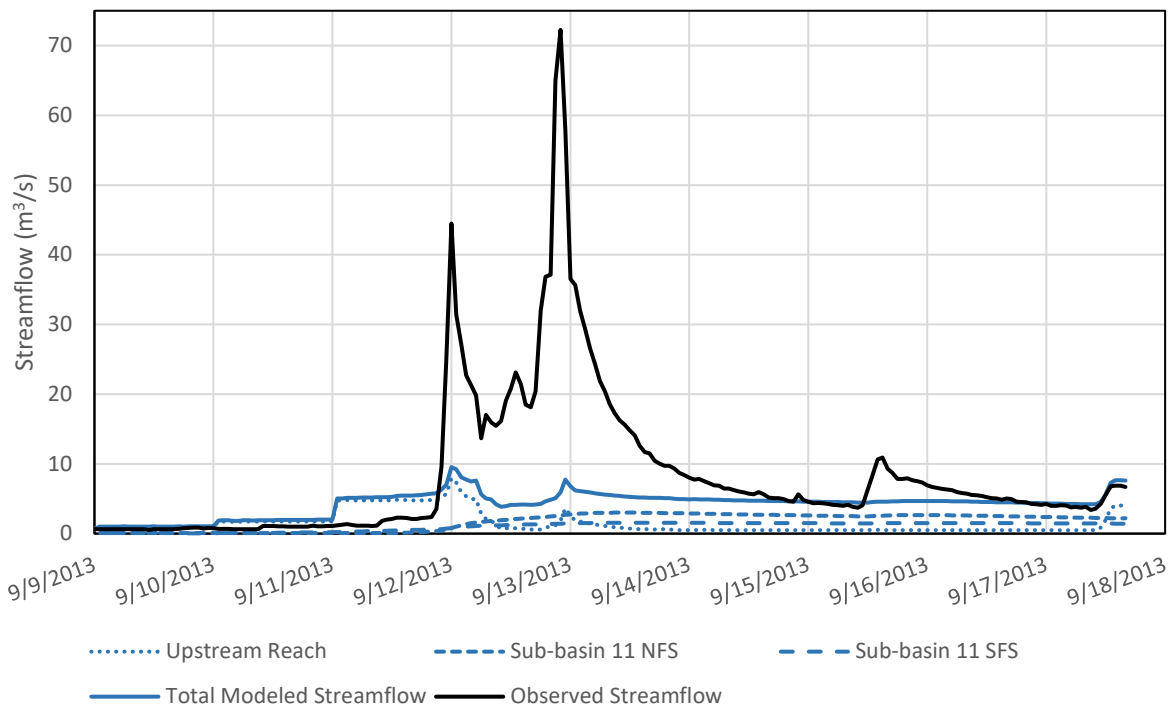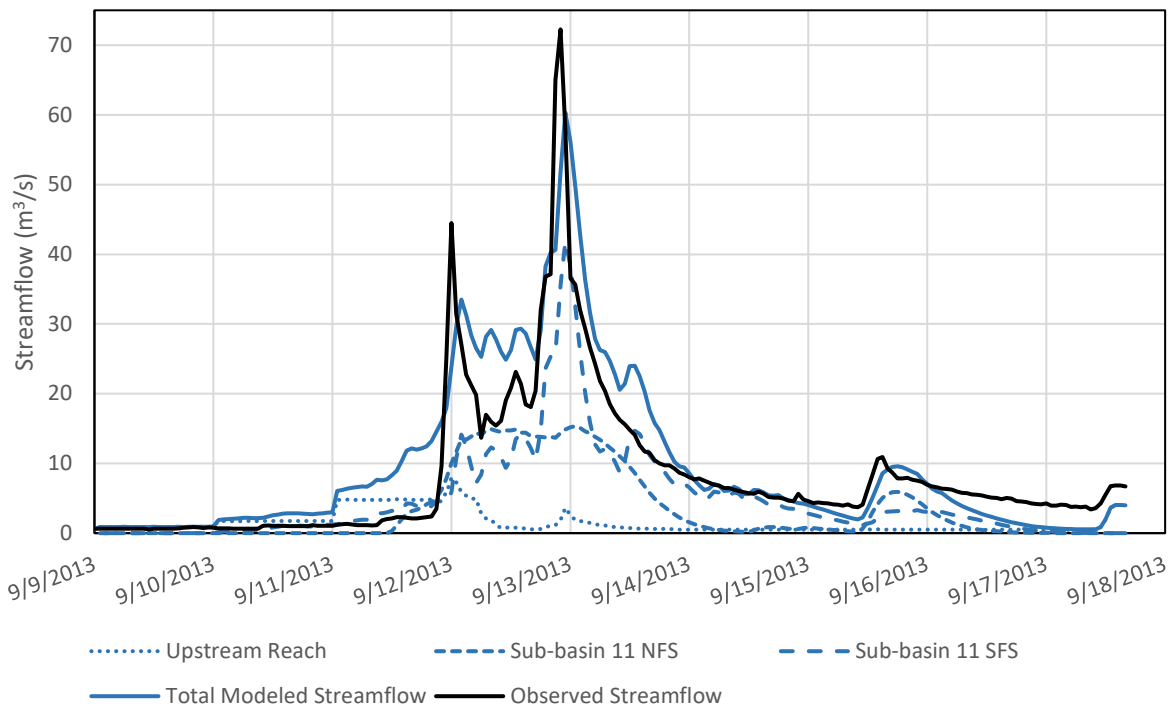

FIGURE 14. *Comparison of modeled streamflow and observed streamflow at the BOCELSCO stream gauge location when the model is forced to emphasize saturation-excess runoff.*

4. EXTENDING RESEARCH TO OTHER BASINS

During the reporting period, a foundation was developed for extending the project to other Front Range basins and extreme events. The primary criteria for selecting additional basins and events were: (1) production of record streamflow, (2) location in the Colorado Front Range, and (3) availability of streamflow and precipitation data. The final basins selected are:

- North Fork of the Big Thompson River at Drake
- Big Thompson River above Estes Park
- South Boulder Creek at Eldorado Springs (discussed in this report)
- Bear Creek at Evergreen

- Cheyenne Creek at Evans Avenue

In the second year, we plan to simulate the September 2013 storm for all these basins because data are most readily available for this storm. In addition, the June 1997 storm will be simulated for Cheyenne Creek, and the July 1976 storm will be modeled for the North Fork of the Big Thompson River. Streamflow data for the 1976 storm are incomplete, so this case will be given lowest priority. Gridded precipitation data have already been obtained for all these basins and events from AWA. The goals of the proposed modeling are: (1) to ensure the proposed modeling methods are generalizable (i.e., applicable to other basins) and (2) to determine whether saturation-excess runoff occurred for other basins and historical extreme events.

We also plan to simulate design storms and compare the proposed methods to Colorado's existing guidelines. The 25-year, 100-year, 1,000-year, and probable maximum precipitation (PMP) events were identified as appropriate events for such comparisons.

5. PRIMARY CONCLUSIONS

This study aimed to determine the runoff production mechanism active during the September 2013 flood in South Boulder Creek and to develop a modeling approach that simulates this mechanism. Although the results presented in this report are preliminary, and the project will continue into a second year under different sponsorship, the results support three primary conclusions:

1. Saturation-excess runoff production was the dominant runoff production mechanism during the September 2013 flood. This result is supported by in-situ soil moisture observations from the Front Range region that show saturation occurring first at the bottom of the soil layer and then proceeding towards the surface. This behavior suggests the soil's limited storage capacity was an important factor in producing runoff and that saturation occurred from below.

2. Runoff production occurred primarily on SFS (and not NFS) for the September 2013 flood. This result is also supported by the available soil moisture observations. A strong majority of available sites that reached saturation (ten out of 14) occurred on SFS. The

primary reasons for this behavior are unclear. However, SFS have lower vegetation density, which is expected to cause less interception and more water reaching the soil as throughfall. In addition, the lower vegetation density may reduce the weathering of bedrock, producing thinner soils and less soil storage. The reduced weathering might also reduce the percolation to the groundwater, which would promote saturation and runoff.

3. A model developed using the SMA method in HEC-HMS can reproduce these observed behaviors in South Boulder Creek. The developed model produces runoff because the soil storage nearly reaches saturation, which causes very low infiltration capacities and runoff to occur. The model also produces runoff on SFS but not on NFS as expected from the soil moisture observations. When the soil's limited storage capacity is neglected (i.e., the model emphasizes infiltration-excess runoff), the model does not produce runoff. When the soil's maximum infiltration capacity is increased (i.e., the model emphasizes saturation-excess runoff), the model results remain similar to the base scenario.

These preliminary results will be tested further in the second year of the project. Specifically, models will be built for four other basins in the Colorado Front Range, and their behavior will be examined for the September 2013 event and other historical events. We anticipate the future results will be available in a final report from the Mountain-Plains Consortium as well as journal publications and Colorado Dam Safety documents.

7. REFERENCES

Anderson, S.P., R.S. Anderson, G.E. Tucker, D.P. Dethier. 2013. Critical zone evolution: Climate and exhumation in the Colorado Front Range. *Geological Society of America*. 33: 1-18

Anderson, S.P., E. Hinckley, N. Rock. (2018). "CZO Dataset: Gordon Gulch: Lower - Soil Temperature, Soil Moisture (2009-2018) - Soil Sensors (GGL_SPTran_SLTmpSLMist_Array)." Retrieved from http://criticalzone.org/boulder/data/dataset/2426/

Andreassian, V., A. Oddos, C. Michel, F. Anctil, C. Perrin, C. Loumagne,. 2004. Impact of spatial aggregation of inputs and parameters on the efficiency of rainfall-runoff models: A theoretical study using chimera watersheds. *Water Resources Research*. 40: W05209

Bell, J. E., M. A. Palecki, C. B. Baker, W. G. Collins, J. H. Lawrimore, R. D. Leeper, M. E. Hall, J. Kochendorfer, T. P. Meyers, T. Wilson, and H. J. Diamond. 2013: U.S. Climate Reference Network soil moisture and temperature observations. *Journal of Hydrometeorology*, 14: 977-988

Chow, Ven Te, 1959, Open-channel Hydraulics, McGraw-Hill Book Company, p. 112-113

Clark, C.O. 1945. Storage and the unit hydrograph: *Transactions: American Society of Civil Engineers*. 110: 1419-1488

Coe, J.A., J.W. Kean, J.W. Godt, R.L. Baum, E.S. Jones, D. Gochis, G.S. Anderson, 2014. New insights into debris-flow hazards from an extraordinary event in the Colorado Front Range. *Geological Society of America*. 24(10): 4-10

Diamond, H. J., T. R. Karl, M. A. Palecki, C. B. Baker, J. E. Bell, R. D. Leeper, D. R. Easterling, J. H. Lawrimore, T. P. Meyers, M. R. Helfert, G. Goodge, P. W. Thorne. 2013: *U.S. Climate Reference Network after one decade of operations: status and assessment. Bulletin of American Meteorological Society*. 94: 489-498.

Division of Water Resources (DWR) Dam Safety Branch. 2014. Report of September 2013 Little Thompson River Flooding and Big Elk Meadows Dam Failures. *Colorado State Publications Library*.

DWR Dam Safety Branch, 2015, Carriage Hills No. 2 Dam (DAMID 040110) September 2013 Dam Failure Forensic Investigation Report. *Colorado State Publications Library*

Domenico, P.A., and F.W. Schwartz. 1990. Physical and Chemical Hydrogeology. John Wiley & Sons, Inc. New York

Dunne, Thomas and Leopold, Luna, *Water in Environmental Planning*, San Francisco: W.H. Freeman, 1978

Dunne, Thomas. 1978. Field studies of hillslope flow processes. *Hillslope Hydrology*. Chapter 7: 227-293, John Wiley & Sons, London

Ebel, Brian A., F.K Rengers, and G.E. Tucker. 2015, Aspect-dependent soil saturation and insight into debris-flow initiation during extreme rainfall in the Colorado Front Range, *Geology* 43 (8): 659-662

Federal Emergency Management Agency (FEMA), October 16, 2013. Post-Flood DEM Final, https://geodata.co.gov/#

Feldman, D. Arlen, 2000. Hydrologic Modeling System HEC-HMS Technical Reference Manual. U.S. Army Corps of Engineers

Fleming, Matt and Vincent Neary. 2004. Continuous Hydrologic Modeling Study with the Hydrologic Modeling System. *Journal of Hydrologic Engineering*. 9(3): 175-183

Flügel, W.A. 1995. Hydrological Response Units Delineated by GIS analyses for regional hydrological modelling of a mesoscale catchment in Germany. *Hydrological Processes* 9(3-4): 237-482

Grimm, M.M., E.E. Wohl, and R.D. Jarrett, 1995, Coarse-sediment distribution as evidence of an elevation limit for flash flooding, Bear Creek, Colorado. *Geomorphology*. 14: 199-210.

Green, W.H. and G. Ampt. 1911. Studies of soil physics, part I the flow of air and water through soils. *Journal of Agricultural Sciences*. 4: 1-24.

Jacobs, Inc., 2014, "Hydrologic evaluation of the Big Thompson watershed: Post September 2013 flood event," Report to Colorado Department of Transportation Region 4 Flood Recovery Office.

Jarrett, Robert D., and Costa, John E. 1988. Evaluation of the flood hydrology in the Colorado Front Range using precipitation, streamflow, and paleflood data for the Big Thompson River Basin, Water Resources Investigations Report 87-4117, United States Geological Survey

Kellogg, K.S., R.R. Shroba, B. Bryant, and W.R. Premo. 2008. Geologic map of the Denver West 30' x 60' quadrangle, north-central Colorado: U.S. Geological Survey, Scientific Investigations Map SIM-3000, scale 1:100,000.

Linsley, R.K., M.A. Kohler, J.L.H. Paulhus. 1958, Hydrology for Engineers, McGraw-Hill Book Company, New York. p. 152-155

Livers, Bridget and Ellen Wohl. 2015. An evaluation of stream characteristics in glacial versus fluvial process domains in the Colorado Front Range. *Geomorphology*. 231: 72-82

MacDonald, Lee H., and Stednick, John D. 2003. *Forests and Water: A State-of-the-Art Review for Colorado*. Colorado Water Institute, Completion Report No. 196, Colorado State University, Fort Collins, CO.

MetStat. Storm Precipitation Analysis System (SPAS). https://metstat.com/storm-analysis/spas/ (accessed August 16, 2018)

NCEP/EMC. 2009. NLDAS Mosaic Land Surface Model L4 Hourly 0.125 x 0.125 degree V002, Edited by David Mocko, NASA/GSFC/HSL, Greenbelt, Maryland, USA, Goddard Earth Sciences Data and Information Services Center (GES DISC), Accessed: 7/30/2018. https://disc.gsfc.nasa.gov/datasets/NLDAS_MOS0125_H_V002/summary.

Perry, M.A., J. Franz, C. Dick, B. Kappel. 2017. Advances in Flood Hydrology for Modeling High Elevation Mountain Basins in Colorado with Applications to the Gross Dam Enlargement Study. Association of State Dam Safety Officials Dam Safety Conference. Philadelphia, Pennsylvania.

Rawls, W.J., D.L Brakensiek, and N. Miller. 1983, Green-Ampt Infiltration Parameters from Soils Data, *Journal of Hydraulic Engineering.* 109(1): 62-70

Rengers, F.K, L.A. McGuire, J.A. Coe, J.W. Kean, R.L. Baum, D.M. Staley, J.W. Godt. 2016. The influence of vegetation on debris-flow initiation during extreme rainfall in the northern Colorado Front Range. *Geology*. 44(10): 823-826.

Sabol, George V., 2008, Hydrologic Basin Response Parameter Estimation Guidelines, State of Colorado, Office of the State Engineer, Dam Safety Branch.

Saxton, K.E., and W.J. Rawls. 2006. Soil Water Characteristic Estimates by Texture and Organic Matter for Hydrologic Solutions. *Soil Science Society of America Journal*. 70: 1569-1578.

Sherman, L.K., 1932. Stream Flow from Rainfall by the Unit Graph Method. *Engineering News Record.* 108: 501-505

Sternberg, P.D., M.A. Anderson, R.C. Graham, J.L. Beyers, K.R. Tice. 1996. Root distribution and seasonal water status in weathered granitic bedrock under chaparral. *Geoderma*. 72: 89-98.

Traff, D.C., J.D. Niemann, S.A. Middlekauff, B.M. Lehman. 2015. Effects of Woody Vegetation on Shallow Soil Moisture at a Semiarid Montane Catchment. *Ecohydrology.* 8: 935-947.

United States Forest Service. *BOW 16-14*. October, 25, 1938. Aerial Photographs of Colorado Collection. https://cudl.colorado.edu/luna/servlet/detail/UCBOULDERCB1~17~17~35911~103285: BOW-16-14?sort=sortorder%2Cdate&qvq=w4s:/who%2FUnited%2BStates%2BForest%2BServic

e%2Fwhen%2F10%25252F25%25252F1938;sort:sortorder%2Cdate;lc:UCBOULDERC
B1~17~17&mi=87&trs=186

US Army Corps of Engineers. 2016. Hydrologic Modeling System HEC-HMS. Version 4.2.1

Witty, J.H., R.C. Graham, K.R. Hubbert, J.A. Doolittle, J.A. Wald. 2003. Contributions of water supply from the weathered bedrock zone to forest soil quality. *Geoderma*. 114: 389-400

Whipkey, Ronald Z. 1965. Subsurface Stormflow from Forested Slopes. *International Association of Scientific Hydrology. Bulletin.* 10 (2): 74–85.

Xia, Y., K. Mitchell, M. Ek, J. Sheffield, B. Cosgrove, E. Wood, L. Luo, C. Alonge, H. Wei, J. Meng, B. Livneh, D. Lettenmaier, V. Koren, Q. Duan, K. Mo, Y. Fan, and D. Mocko. 2012. Continental-scale water and energy flux analysis and validation for the North American Land Data Assimilation System project phase 2 (NLDAS-2): 1. Intercomparison and application of model products, *Journal Geophysical Research*. 117: D03109.

Zhang, Z., V. Koren, M. Smith, S. Reed, D. Wang. 2004. Use of Next Generation Weather Radar Data and Basin Disaggregation to Improve Continuous Hydrograph Simulations, *Journal of Hydrology*. 9(2): 103-115.